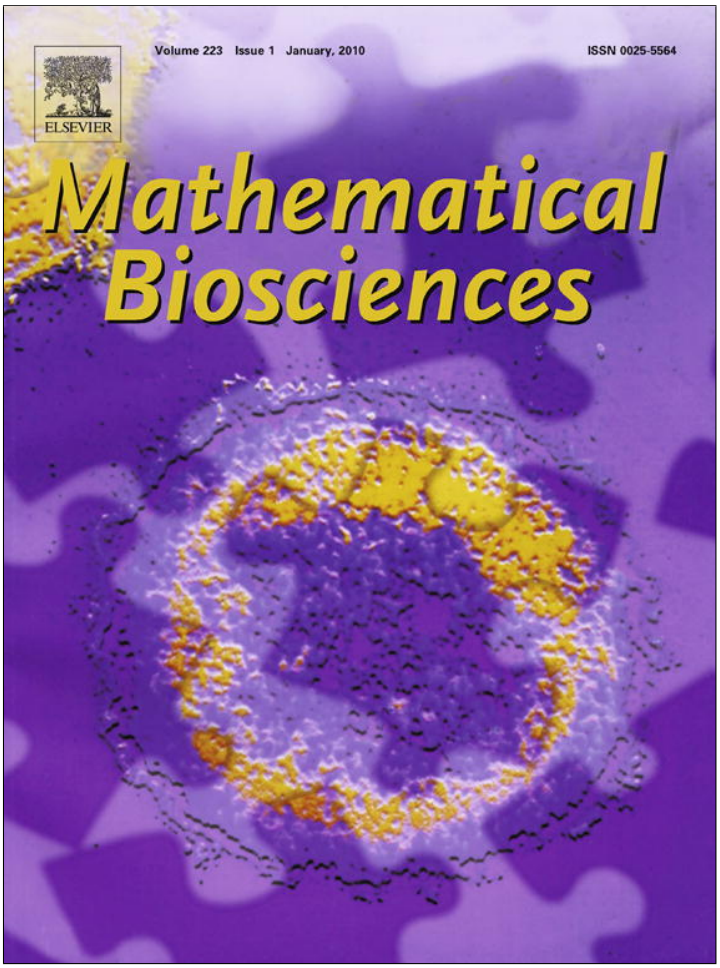

Mathematical Biosciences 223 (2010) 32–46

Contents lists available at ScienceDirect

Mathematical Biosciences

journal homepage: www.elsevier.com/locate/mbs

Stochastic eco-epidemiological model of dengue disease transmission by *Aedes aegypti* mosquito

M. Otero *, H.G. Solari

Departamento de Física, Facultad de Ciencias Exactas y Naturales, Universidad de Buenos Aires, Pabellón 1 Ciudad Universitaria, 1428 Ciudad Autónoma de Buenos Aires, Argentina

ARTICLE INFO

Article history:
Received 9 January 2009
Received in revised form 9 October 2009
Accepted 15 October 2009
Available online 25 October 2009

Keywords:
Eco-epidemiology
Aedes aegypti
Stochastic models
Dengue

ABSTRACT

We present a stochastic dynamical model for the transmission of dengue that takes into account seasonal and spatial dynamics of the vector *Aedes aegypti*. It describes disease dynamics triggered by the arrival of infected people in a city. We show that the probability of an epidemic outbreak depends on seasonal variation in temperature and on the availability of breeding sites. We also show that the arrival date of an infected human in a susceptible population dramatically affects the distribution of the final size of epidemics and that early outbreaks have a low probability. However, early outbreaks are likely to produce large epidemics because they have a longer time to evolve before the winter extinction of vectors. Our model could be used to estimate the risk and final size of epidemic outbreaks in regions with seasonal climatic variations.

1. Introduction

Arboviruses is a shortened name given to arthropod-borne viruses from various families which are transmitted by arthropods. Some Arboviruses are able to cause re-emergent diseases such as St. Louis Encephalitis, Chikungunya, Dengue, Ross River disease, West Nile, Yellow Fever, Equine Encephalitis, etc. [1]. Arthropods are able to transmit the virus upon biting the host, allowing the virus to enter the host's bloodstream. The virus replicates in the vector but usually does not harm it. In the mosquito-borne diseases, the virus establishes a persistent infection in the mosquito salivary glands and there is sufficient virus in the saliva to infect another host during feeding. Each arbovirus usually grows only in a limited number of mosquito species. The work presented in this article is focused on mosquito-borne diseases (mainly dengue fever) transmitted by *Aedes aegypti*. This is one of the most efficient mosquito vectors for arboviruses, because it is highly anthropophilic, thrives in close proximity to humans and often lives indoors.

Dengue is spread only by adult females, which require blood to complete oogenesis. During the blood meal the female ingests dengue viruses from an infectious human. The viruses develop within the mosquito and are re-injected in later blood meals into the blood stream of susceptible humans. Dengue is an acute febrile viral disease (with four serotypes of flaviviruses *DEN*1, *DEN*2, *DEN*3 and *DEN*4) which presents headaches, bone, joint and muscular pains, rash and leukopenia as symptoms. Dengue epidemics were reported throughout the 19th and 20th centuries in the Americas, southern Europe, northern Africa, the eastern Mediterranean, Asia, Australia and on various islands in the Indian Ocean, Central Pacific and Caribbean [2].

The history of dengue in Argentina began as early as in 1916 when an epidemic affected the cities of Concordia and Paraná. In 1947 the Pan American Health Organization (PHO) led a continental mosquito eradication program and by 1967 the mosquito was considered to be eradicated in Argentina. The mosquito was detected again in 1986 and since 1997 several epidemic outbreaks took place in the northwestern and northeastern regions of the country. A brief history of dengue epidemics in Argentina is found in Appendix A.

Nowadays *A. aegypti* is a permanent inhabitant of the city of Buenos Aires [3–5]. Every summer there is a potential risk of dengue virus transmission because of the arrival of viremic people from Bolivia, Paraguay, Brazil and other endemic countries. However, no autochthonous cases of the disease have been detected until present [5], but in the last years some clinical studies confirmed dengue infection in people arriving from neighboring endemic countries [6]. Therefore, the development of mathematical models which permit the estimation of the probability of an epidemic outbreak and its final size has become a matter of sanitary necessity.

The first model of dengue was performed by Newton and Reiter in 1992 [7]. They developed a deterministic model in which the populations of hosts and vectors were divided into subpopulations representing disease status and the flow between subpopulations was described by differential equations. Several deterministic models have been developed taking into account different possible aspects of the disease: constant human population and variable

* Corresponding author.
E-mail addresses: mjotero@df.uba.ar (M. Otero), solari@df.uba.ar (H.G. Solari).

0025-5564/$ - see front matter © 2009 Elsevier Inc. All rights reserved.
doi:10.1016/j.mbs.2009.10.005

vector population [8], variable human population size [9], vertical and mechanical transmission in the vector population [10], seasonally varying parameters and presence of two simultaneous dengue serotypes [11], age structure in the human population [12] and presence of two serotypes of dengue at separated intervals of time [13]. In addition, in 2006 Tran and Raffy proposed a spatial and temporal dynamical model based on diffusion equations using remote-sensing data [14].

There are also other approaches. Focks et al. developed a stochastic model that describes the daily dynamics of dengue virus transmission in an urban environment based on the simulation of a human population growing in response to country- and age-specific birth and death rates [15]. Santos et al. developed a periodically forced two-dimensional cellular automata model that describes complex features of the disease taking into account external seasonality (rainfall) and human and mosquito mobility [16].

Our proposal in this article is the third in a series of minimalist stochastic models. The first describes the seasonal dynamics of *A. aegypti* populations in a homogeneous environment [17]. The second one describes the *A. aegypti* dispersal driven by the availability of oviposition sites in an urban environment [18]. This new model takes into account the seasonal and spatial dynamics of the vectors and describes the disease dynamics triggered by the arrival of viremic people in a city.

Our main goal is the development of a mathematical tool that allows the study of different epidemic scenarios in an urban environment, the estimation of the epidemic risk and the study of the growth and final size of an epidemic outbreak due to the spatial dynamics of the vector. A particular aim of the work is the estimation of dengue epidemic risk in the city of Buenos Aires, Argentina.

Populations of hosts (Humans) and vectors (*A. aegypti*) were divided into subpopulations representing disease status: susceptible (S), exposed (E) and infectious (I) for adult female vectors, and susceptible (S), exposed (E), infectious (I) and removed (R) for the human population. The population of adult male mosquitoes is not taken into account explicitly and we consider that, on average, one half of the emerging adults are females [19]. Three kinds of females were considered: adult females in their first gonotrophic cycle (*A*1 females), females in subsequent gonotrophic cycles (*A*2 females) and flyers (*F*), which are the adult females that have already finished their gonotrophic cycles and fly in order to deposit their eggs.

The following sections will describe the populations and events of the stochastic transmission model (Section 2), the mathematical description of the stochastic model (Section 3), the parameters, initial values and boundary conditions (Section 4), results and discussion (Section 5), the transcription of the dengue model into a yellow fever model, the choice of dengue parameters as well as some minimal computations in the validation direction (Section 6), and finally, summary and conclusions (Section 7).

2. Populations and events of the stochastic transmission model

2.1. Populations of the stochastic process

We consider a two-dimensional space as a mesh of squared patches where the dynamics of the immature stages of the mosquito and the evolution of the disease take place, and where only Flyers can fly from one patch to the next according to a diffusion-like process. We take into account that during the gonotrophic cycles the mosquito dispersal is negligible, and once the gonotrophic cycle ends the female begins to fly, becoming a Flyer in search of oviposition sites. A detailed explanation of the dispersal model has been already presented [18]. In the present work, host movement was not taken into account.

The patch coordinates are given by two indices, i and j, corresponding to the row and column in the mesh. If X_k is a subpopulation in the stage k, then $X_k(i,j)$ is the X_k subpopulation in the patch of coordinates (i,j).

The transmission of only one serotype of virus was considered, and mechanical transmission (i.e., without amplification of the virus in the vector) was not taken into account. The populations of both hosts (Humans) and vectors (*A. aegypti*) were divided into subpopulations representing disease status: S.E.I for the vectors and S.E.I.R for the human population.

Ten different subpopulations for the mosquito were taken into account: three immature subpopulations (eggs $E_{(i,j)}$, larvae $L_{(i,j)}$ and pupae $P_{(i,j)}$), and seven adult subpopulations (female adults not having laid eggs $A1_{(i,j)}$, susceptible flyers $Fs_{(i,j)}$, exposed flyers $Fe_{(i,j)}$, infectious flyers $Fi_{(i,j)}$ and female adults having laid eggs according to their disease status: susceptible $A2s_{(i,j)}$, exposed $A2e_{(i,j)}$ and infectious $A2i_{(i,j)}$).

$A1_{(i,j)}$ are always susceptible because we neglect the vertical transmission of the virus. After a blood meal, $A1_{(i,j)}$ become either susceptible $Fs_{(i,j)}$ or exposed $Fe_{(i,j)}$, depending on the disease status of the host. If the host is infectious, $A1_{(i,j)}$ become $Fe_{(i,j)}$ but if the host is not infectious, then $A1_{(i,j)}$ become $Fs_{(i,j)}$.

The human population $Nh_{(i,j)}$ was split into four different subpopulations according to the disease status: susceptible humans $Hs_{(i,j)}$, exposed humans $He_{(i,j)}$, infectious humans $Hi_{(i,j)}$ and removed humans $Hr_{(i,j)}$.

The evolution of all the 14 subpopulations is affected by 38 different possible events. Events occur at rates that depend on subpopulation values and some of them also on temperature, which is a function of time since it changes over the course of the year seasonally [17,18]. Hence, the dependence on temperature introduces a time dependence in the event rates. A brief description of the temperature model is presented in Appendix B.

2.2. Events related to immature stages

Pre-imaginal stages of domestic *A. aegypti* develop in artificial containers of small volume such as buckets, jars, flasks, bottles and flower vases [20]. The natural regulation of *A. aegypti* populations is due to intra-specific competition for food and other resources in the larval stage. This regulation was incorporated into the model as a density-dependent transition probability which introduces the necessary non-linearities that prevent a Malthusian growth of the population. This effect was incorporated as a nonlinear correction to the temperature-dependent larval mortality.

Then, larval mortality can be written as:

$$\omega_3(L_{(i,j)}) = mlL_{(i,j)} + \alpha L_{(i,j)} * (L_{(i,j)} - 1) \tag{1}$$

where the value of α can be further decomposed as

$$\alpha = \alpha_0 / BS_{(i,j)} \tag{2}$$

with α_0 associated with the carrying capacity of one (standardized) breeding site and $BS_{(i,j)}$ being the density of breeding sites in the (i,j) patch [17,18].

Table 1 summarizes the events and rates related to immature stages of the mosquito during their first gonotrophic cycle. The construction of the transition rates and the choice of model parameters related to the mosquito biology, such as mortality of eggs (**me**), hatching rate (**elr**), mortality of larvae (**ml**), density-dependent mortality of larvae (**α**), pupation rate (**lpr**), mortality of pupae (**mp**), pupae into adults development coefficient (**par**), and emergence factor (**ef**), have been previously described in detail [17,18].

Table 1
Event type, effects on the populations and transition rates for the developmental model. The coefficients are **me**: mortality of eggs; **elr**: hatching rate; **ml**: mortality of larvae; **α**: density-dependent mortality of larvae; **lpr**: pupation rate; **mp**: mortality of pupae; **par**: pupae into adults development coefficient; **ef**: emergence factor. The values of the coefficients are available in Section 4.

Event	Effect	Transition rate
(1) Egg death	$E_{(i,j)} \to E_{(i,j)} - 1$	$w_1 = me * E_{(i,j)}$
(2) Egg hatching	$E_{(i,j)} \to E_{(i,j)} - 1$ $L_{(i,j)} \to L_{(i,j)} + 1$	$w_2 = elr * E_{(i,j)}$
(3) Larval death	$L_{(i,j)} \to L_{(i,j)} - 1$	$w_3 = ml * L_{(i,j)} + \alpha * L_{(i,j)} * (L_{(i,j)} - 1)$
(4) Pupation	$L_{(i,j)} \to L_{(i,j)} - 1$ $P_{(i,j)} \to P_{(i,j)} + 1$	$w_4 = lpr * L_{(i,j)}$
(5) Pupal death	$P_{(i,j)} \to P_{(i,j)} - 1$	$w_5 = (mp + par * (1 - (ef/2))) * P_{(i,j)}$
(6) Adult emergence	$P_{(i,j)} \to P_{(i,j)} - 1$ $A1_{(i,j)} \to A1_{(i,j)} + 1$	$w_6 = par * (ef/2) * P_{(i,j)}$

2.3. Local events related to the adult stage

As we have already explained in Section 1, *A. aegypti* females require blood to complete their gonotrophic cycles. In this process, the female may ingest viruses with the blood meal from an infectious human during its Viremic Period (**VP**). The viruses develop within the mosquito during the Extrinsic Incubation Period (**EIP**) and are then re-injected into the blood stream of a new susceptible human in later blood meals. The virus in the exposed human develops during the Intrinsic Incubation Period (**IIP**) and then begins to circulate in the blood stream, making the human infectious. The flow from susceptible to exposed subpopulations (in the vector and the host) depends not only on the contact between vector and host but also on the transmission probabilities of the virus: the transmission probability from host to vector (**ahv**) and the transmission probability from vector to host (**avh**).

Local events related to the adult stage are shown in Tables 2–5. Table 2 summarizes the events and rates related to adults during their first gonotrophic cycle and related to oviposition by flyers according to their disease status. Tables 3 and 4 summarize the events and rates related to human contagion, *A*2 gonotrophic cycles and $A2e_{(i,j)}$ and $Fe_{(i,j)}$ that become infectious. Table 5 summarizes the events and rates related to the death of *A*2 and *F*.

2.4. Events related to flyer dispersal

The development of *A. aegypti* requires resting sites, oviposition sites, nectar and blood resources. Different levels of urbanization might be associated with differences in the availability of these resources or the connectivity between patches with resources. Less mosquito activity was observed in more urbanized areas with higher density of apartments and/or human population density. In contrast, more activity was observed in less urbanized areas with higher house density and/or closer to industrial sites [21].

One open question about *A. aegypti* dispersal is the motivation of the flight. In fact, some experimental results and observational studies show that *A. aegypti* dispersal is driven by the availability of oviposition sites [22–24]. According to these observations, we considered that only $F_{(i,j)}$ can fly from patch to patch in search of oviposition sites. Flyer dispersal events correspond to event numbers n from 26 to 31. The implementation of flyer dispersal has been described previously [18].

The general rate of the dispersal event is given by:

$$w_n = \beta * F_{(i,j)} \tag{3}$$

where n is the event number $(n = 26, 27, \ldots, 31)$, β is the dispersal coefficient and $F_{(i,j)}$ is the Flyer population which can be susceptible $Fs_{(i,j)}$, exposed $Fe_{(i,j)}$ or infectious $Fi_{(i,j)}$.

The dispersal coefficient β can be written as

$$\beta = \begin{cases} 0 & \text{if the patches are disjoint} \\ diff/d_{ij}^2 & \text{if the patches have at least a common point} \end{cases} \tag{4}$$

where d_{ij} is the distance between the centers of the patches and **diff** is a diffusion-like coefficient so that dispersal is compatible with a diffusion-like process [18].

2.5. Events related to the human population

Table 6 summarizes the events and rates in which humans are involved. Human contagion has been already described in Table 4 and the evolution of the disease in humans is described in Section 2.3. The human population was fluctuating but balanced, meaning that the birth coefficient was considered equal to the mortality coefficient (**mh**).

3. Mathematical description of the stochastic model

The evolution of the subpopulations is modelled by a state-dependent Poisson process [25,26] where the probability of the state:

Table 2
Event type, effects on the subpopulations and transition rates for the developmental model. The coefficients are **ma**: mortality of adults; **cycle1**: gonotrophic cycle coefficient (number of daily cycles) for adult females in stages *A*1; **ahv**: transmission probability from host to vector; $\mathbf{ovr}_{(i,j)}$: oviposition rate by flyers in the (i, j) patch; **egn**: average number of eggs laid in an oviposition. The values of the coefficients are available in Section 4.

Event	Effect	Transition rate
(7) Adults 1 death	$A1_{(i,j)} \to A1_{(i,j)} - 1$	$w_7 = ma * A1_{(i,j)}$
(8) I Gonotrophic cycle with virus exposure	$A1_{(i,j)} \to A1_{(i,j)} - 1$ $Fe_{(i,j)} \to Fe_{(i,j)} + 1$	$w_8 = cycle1 * A1_{(i,j)} * (Hi_{(i,j)}/Nh_{(i,j)}) * ahv$
(9) I Gonotrophic cycle without virus exposure	$A1_{(i,j)} \to A1_{(i,j)} - 1$ $Fs_{(i,j)} \to Fs_{(i,j)} + 1$	$w_9 = cycle1 * A1_{(i,j)} * (((Nh_{(i,j)} - Hi_{(i,j)})/Nh_{(i,j)}) + (1 - ahv) * (Hi_{(i,j)}/Nh_{(i,j)}))$
(10) Oviposition of susceptible flyers	$E_{(i,j)} \to E_{(i,j)} + egn$ $Fs_{(i,j)} \to Fs_{(i,j)} - 1$ $A2s_{(i,j)} \to A2s_{(i,j)} + 1$	$w_{10} = ovr_{(i,j)} * Fs_{(i,j)}$
(11) Oviposition of exposed flyers	$E_{(i,j)} \to E_{(i,j)} + egn$ $Fe_{(i,j)} \to Fe_{(i,j)} - 1$ $A2e_{(i,j)} \to A2e_{(i,j)} + 1$	$w_{11} = ovr_{(i,j)} * Fe_{(i,j)}$
(12) Oviposition of infected flyers	$E_{(i,j)} \to E_{(i,j)} + egn$ $Fi_{(i,j)} \to Fi_{(i,j)} - 1$ $A2i_{(i,j)} \to A2i_{(i,j)} + 1$	$w_{12} = ovr_{(i,j)} * Fi_{(i,j)}$

Table 3
Event type, effects on the subpopulations and transition rates for the developmental model. The coefficients are **cycle2**: gonotrophic cycle coefficient (number of daily cycles) for adult females in stages *A2*; **ahv**: transmission probability from host to vector. The values of the coefficients are available in Section 4.

Event	Effect	Transition rate
(13) II Gonotrophic cycle of susceptible Adults 2 with virus exposure	$A2s_{(i,j)} \to A2s_{(i,j)} - 1$ $Fe_{(i,j)} \to Fe_{(i,j)} + 1$	$w_{13} = cycle2 * A2s_{(i,j)} * (Hi_{(i,j)}/Nh_{(i,j)}) * ah\nu$
(14) II Gonotrophic cycle of susceptible Adults 2 without virus exposure	$A2s_{(i,j)} \to A1_{(i,j)} - 1$ $Fs_{(i,j)} \to Fs_{(i,j)} + 1$	$w_{14} = cycle2 * A2s_{(i,j)} * (((Nh_{(i,j)} - Hi_{(i,j)})/Nh_{(i,j)}) + (1 - ah\nu)ast(Hi_{(i,j)}/Nh_{(i,j)}))$
(15) II Gonotrophic cycle of exposed Adults 2	$A2e_{(i,j)} \to A2e_{(i,j)} - 1$ $Fe_{(i,j)} \to Fe_{(i,j)} + 1$	$w_{15} = cycle2 * A2e_{(i,j)}$

Table 4
Event type, effects on the subpopulations and transition rates for the developmental model. The coefficients are **cycle2**: gonotrophic cycle coefficient (number of daily cycles) for adult females in stages *A2*; $\mathbf{ovr}_{(i,j)}$: oviposition rate by flyers in the (i,j) patch; **avh**: transmission probability from vector to host; **EIP**: extrinsic incubation period. The values of the coefficients are available in Section 4.

Event	Effect	Transition rate
(16) Exposed adults 2 becoming infectious	$A2e_{(i,j)} \to A2e_{(i,j)} - 1$ $A2i_{(i,j)} \to A2i_{(i,j)} + 1$	$w_{16} = (1/(EIP - (1/ovr_{(i,j)}))*)A2e_{(i,j)}$
(17) Exposed flyers becoming infectious	$Fe_{(i,j)} \to Fe_{(i,j)} - 1$ $Fi_{(i,j)} \to Fi_{(i,j)} + 1$	$w_{17} = (1/(EIP - (1/ovr_{(i,j)}))*)Fe_{(i,j)}$
(18) II Gonotrophic cycle of infectious Adults 2 with human contagion	$A2i_{(i,j)} \to A2i_{(i,j)} - 1$ $Fi_{(i,j)} \to Fi_{(i,j)} + 1$ $Hs_{(i,j)} \to Hs_{(i,j)} - 1$ $He_{(i,j)} \to He_{(i,j)} + 1$	$w_{18} = cycle2 * A2i_{(i,j)} * (Hs_{(i,j)}/Nh_{(i,j)}) * a\nu h$
(19) II Gonotrophic cycle of infectious Adults 2 without human contagion	$A2i_{(i,j)} \to A2i_{(i,j)} - 1$ $Fi_{(i,j)} \to Fi_{(i,j)} + 1$	$w_{19} = cycle2 * A2i_{(i,j)} * (((Nh_{(i,j)} - Hs_{(i,j)})/Nh_{(i,j)}) + (1 - a\nu h) * (Hs_{(i,j)}/Nh_{(i,j)}))$

Table 5
Event type, effects on the subpopulations and transition rates for the developmental model. The coefficients are **ma**: adult mortality. The values of the coefficients are available in Section 4.

Event	Effect	Transition rate
(20) Susceptible flyer death	$Fs_{(i,j)} \to Fs_{(i,j)} - 1$	$w_{20} = ma * Fs_{(i,j)}$
(21) Exposed flyer death	$Fe_{(i,j)} \to Fe_{(i,j)} - 1$	$w_{21} = ma * Fe_{(i,j)}$
(22) Infectious flyer death	$Fi_{(i,j)} \to Fi_{(i,j)} - 1$	$w_{22} = ma * Fi_{(i,j)}$
(23) Susceptible adult 2 death	$A2s_{(i,j)} \to A2s_{(i,j)} - 1$	$w_{23} = ma * A2s_{(i,j)}$
(24) Exposed adult 2 death	$A2e_{(i,j)} \to A2e_{(i,j)} - 1$	$w_{24} = ma * A2e_{(i,j)}$
(25) Infectious adult 2 death	$A2i_{(i,j)} \to A2i_{(i,j)} - 1$	$w_{25} = ma * A2i_{(i,j)}$

$$(E, L, P, A1, A2s, A2e, A2i, Fs, Fe, Fi, Hs, He, Hi.Hr)_{(i,j)}$$

evolves in time following a Kolmogorov forward equation that can be constructed directly from the information collected in Tables 1–6 and in Eq. (4). Fig. 1 shows the subpopulations of vector populations and the events which affect these populations collected in Tables 1–5 and Eq. (4). Fig. 2 shows the subpopulations of human populations and the events which affect these populations collected in Tables 4 and 6.

3.1. Deterministic rates approximation for the density-dependent Markov process

We consider X is an integer vector having as entries the populations under consideration, and $e_\alpha, \alpha = 1 \dots \kappa$ the events at which the populations change by a fixed amount Δ_α in a Poisson process with density-dependent rates. Then, a theorem by Kurtz and co-worker [25] allows us to rewrite the stochastic process as:

$$X(t) = X(0) + \sum_{\alpha=1}^{\kappa} \Delta_\alpha Y\left(\int_0^t \omega_\alpha(X(s))ds\right) \tag{5}$$

Table 6
Event type, effects on the subpopulations and transition rates for the developmental model. The coefficients are **mh**: human mortality coefficient; **VP**: human viremic period; **mh**: human mortality coefficient; **IIP**: intrinsic incubation period. The values of the coefficients are available in Section 4.

Event	Effect	Transition rate
(32) Birth of susceptible humans	$Hs_{(i,j)} \to Hs_{(i,j)} + 1$	$w_{32} = mh * Nh_{(i,j)}$
(33) Death of susceptible humans	$Hs_{(i,j)} \to Hs_{(i,j)} - 1$	$w_{33} = mh * Hs_{(i,j)}$
(34) Death of exposed humans	$He_{(i,j)} \to He_{(i,j)} - 1$	$w_{34} = mh * He_{(i,j)}$
(35) Transformation from exposed to viremic	$He_{(i,j)} \to He_{(i,j)} - 1$ $Hi_{(i,j)} \to Hi_{(i,j)} + 1$	$w_{35} = (1/IIP) * He_{(i,j)}$
(36) Death of Infectious humans	$Hi_{(i,j)} \to Hi_{(i,j)} - 1$	$w_{36} = mh * Hi_{(i,j)}$
(37) Removal of infectious humans	$Hi_{(i,j)} \to Hi_{(i,j)} - 1$ $Hr_{(i,j)} \to Hr_{(i,j)} + 1$	$w_{37} = (1/VP) * Hi_{(i,j)}$
(38) Death of removed humans	$Hr_{(i,j)} \to Hr_{(i,j)} - 1$	$w_{38} = mh * Hr_{(i,j)}$

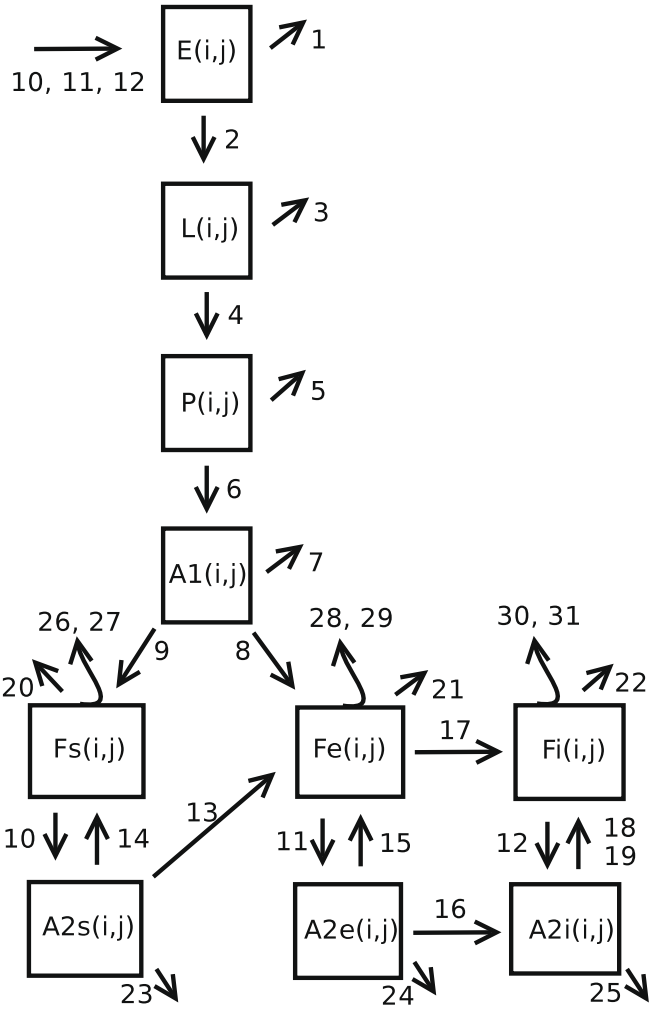

Fig. 1. Populations and events of the stochastic model, where $n = 1, 2, \ldots, 31$ are the event numbers collected in Tables 1–4, Eq. (4) and Table 5. Events 1, 3, 5, 7, 20, 21, 22, 23, 24 and 25 correspond to vector death and events 26–31 correspond to adult dispersal.

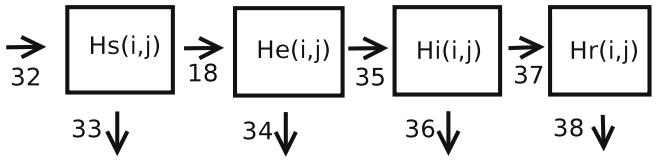

Fig. 2. Populations and events of the stochastic model, 18, 32, 33, ..., 38 are the event numbers collected in Table 4 and in Table 6. Event 32 corresponds to human birth and events 33, 34, 36 and 38 to human death.

where $\omega_\alpha(X(s))$ is the transition rate associated with the event α and $Y(x)$ is a random Poisson process of rate x.

The deterministic rates approximation to the stochastic process represented by Eq. (5) consists in introducing deterministic approximation for the arguments of the Poisson variables $Y(x)$ in Eq. (5) [27,28]. The reason for such a proposal is that the transition rates change at a slower rate than the populations. The number of each kind of event is then approximated by independent Poisson processes with deterministic arguments satisfying a differential equation.

The probability of n_α events of type α having occurred after a time dt is approximated by a Poisson distribution with parameter λ_α. Hence, the probability of the population taking the value

$$X = X_0 + \sum_{\alpha=1}^{\kappa} \Delta_\alpha n_\alpha \tag{6}$$

at a time interval dt after being in the state X_0 is approximated by a product of independent Poisson distributions of the form

$$\text{Probability}(n_1 \ldots n_\kappa, dt/X_0) = \prod_{\alpha=1}^{\kappa} P_\alpha(\lambda_\alpha) \tag{7}$$

and

$$P^{\alpha}_{n_1 \ldots n_E}(\lambda_\alpha) = \exp(-\lambda_\alpha)\frac{\lambda_\alpha^{n_\alpha}}{n_{\alpha!}} \tag{8}$$

whenever $X = X_0 + \sum_{\alpha=1}^{\kappa} \Delta_\alpha n_\alpha$ has no negative entries and

$$P^{\alpha}_{n_1 \ldots n_E}(\lambda_\alpha) = \exp(-\lambda_\alpha)\sum_{i=n_\alpha}^{\infty}\frac{\lambda_\alpha^i}{i!} = 1 - \exp(-\lambda_\alpha)\sum_{i=0}^{n_\alpha - 1}\frac{\lambda_\alpha^i}{i!} \tag{9}$$

if $\{n_i\}$ makes a component in X zero (see [27]).

Finally,

$$d\lambda_\alpha/dt = \langle \omega_\alpha(X) \rangle \tag{10}$$

where the averages are taken self-consistently with the proposed distribution ($\lambda_\alpha(0) = 0$).

The use of the Poisson approximation represents a substantial saving of computer time compared to direct (Monte Carlo) implementations of the stochastic process.

4. Parameters, initial values and boundary conditions

4.1. Parameters related to mosquito biology

The description of the development of the transition rates and the choice of the model parameters related to mosquito biology and dispersal such as mortality of eggs (**me**), hatching rate (**elr**), mortality of larvae (**ml**), density-dependent mortality of larvae (**α**), pupation rate (**lpr**), mortality of pupae (**mp**), pupae into adults development coefficient (**par**), emergence factor (**ef**), mortality of adults (**ma**), gonotrophic cycle coefficients (**cycle1, cycle2**) for adult females in stages $A1$ and $A2$, oviposition rate ($\mathbf{ovr}_{(i,j)}$) by flyers in the (i,j) patch, diffusion-like coefficient (**diff**) and the average number of eggs laid in an oviposition (**egn**) have been previously described in detail [17,18]. A brief description of these parameters and their dependence on temperature is presented in Appendix B.

4.2. Parameters related to arbovirus diseases

Table 7 summarizes the parameter values for the model of dengue fever transmission [7]. No mortality due to the disease was considered because only one serotype of dengue virus was supposed to cause the epidemic outbreaks and the seroprevalence of antibodies in the susceptible population was considered as 0%. Therefore, the human population was considered fluctuating but roughly constant during the outbreak period and the birth coefficient was considered equal to the mortality coefficient $mh = (1/75)\text{years}^{-1}$.

Table 7
Coefficients, symbols and values of the characteristic parameters of dengue disease. The coefficients are **VP**: the human viremic period, **EIP**: the extrinsic incubation period, **IIP**: the intrinsic incubation period, **ahv**: the transmission probability host to vector and **avh**: transmission probability vector to host.

Coefficient	Symbol	value
Intrinsic incubation period	*IIP*	5 days
Extrinsic incubation period	*EIP*	10 days
Human viremic period	*VP*	3 days
Transmission probability host to vector	*ahv*	0.75
Transmission probability vector to host	*avh*	0.75

4.3. Initial values and boundary conditions

Studies performed in the city of Buenos Aires [5,29] have shown a particular spatial distribution of the mosquito and suggest that the extinction of adults and all aquatic forms of the mosquito are common in localized areas of the city, being the egg stage the only one that can survive the winter period. According to these observations, we chose as initial time July 1st, ran the model with different initial egg population values and observed no significant differences in any population numbers provided the mosquito survived until the following favorable season (spring–summer) [17,18]. These results show a very strong regulatory capability of the environment. The carrying capacity of the environment, reflected by the Breeding Site parameter (BS), regulates the mosquito populations, which show little to no memory of the population situation 1 year before. Therefore, we used 10,000 eggs/ha as initial value for the mosquito populations and considered 1 year as transient period.

Many quarters suitable for the mosquito development have a population density lower than the population density of the city (146.3 inhab./ha). Then, we considered as mean population density 100 inhab./ha according to the population densities of the quarters with high mosquito abundance.

The spatial boundary condition takes into account that the probability of the flyers $F_{(i,j)}$ flying away from the region under study was considered equal to the probability of flying into that region, which means a zero average derivative condition. This assumes that the patch is just part of a larger region with the same favorable conditions for the mosquitoes.

5. Results and discussion

5.1. Effect of the date of arrival of one exposed human in the final size of the epidemics

Fig. 3 shows the frequency of the final size of epidemics as a function of the date of arrival of one exposed human in the susceptible human population. By final size of epidemics we understand the total number of susceptible humans who were infected during the epidemic outbreak. We performed the simulations using a grid with 13×13 patches and with a density of breeding sites of 200 BS/patch. We started with 100 susceptible humans and 10,000 mosquito eggs in every patch July 1st and we ran the simulations for 2 years. The seasonal variation of temperature was calculated by using Eq. (16) (see Appendix B). Only the second year of each simulation was analyzed since the first year was considered as transient (see Section 4.3). This procedure was repeated 100 times for 12 different dates of arrival of one exposed human in the susceptible human population in the central patch of the grid during the second year of the simulation. Histograms of the final size of epidemics were constructed using a bin size of 1000.

Fig. 3 shows that no epidemic outbreaks take place during the winter season and that the final size distribution is bimodal (i.e., either no or only a few individuals are infected or else a fairly large proportion of the susceptible population is infected, such as in standard Markovian SIR epidemic models) [26]. Fig. 3 also shows that the date of arrival of the exposed human affects not only the shape but also the center of the distribution.

In order to see more clearly the details of the histograms, Fig. 4 shows the histograms of non-zero final size of epidemics for four different dates of arrival of the exposed human: November 1st, December 1st, January 1st and February 1st. This is, the relative frequency of an epidemic according to the size (binned) conditioned to be a non-zero epidemic. The analysis of the probability of no-development of an epidemic outbreak is discussed in Section 5.2.

Fig. 4 clearly shows that the date of arrival of the exposed human dramatically affects the distribution of the final size of epidemics. If the exposed human is incorporated into the susceptible population on November 1st, the frequency of development of epidemic outbreaks is low but instead the maximum final size is very high reaching almost 62% of the initial susceptible population. That corresponds to a scenario in which the probability of an epidemic

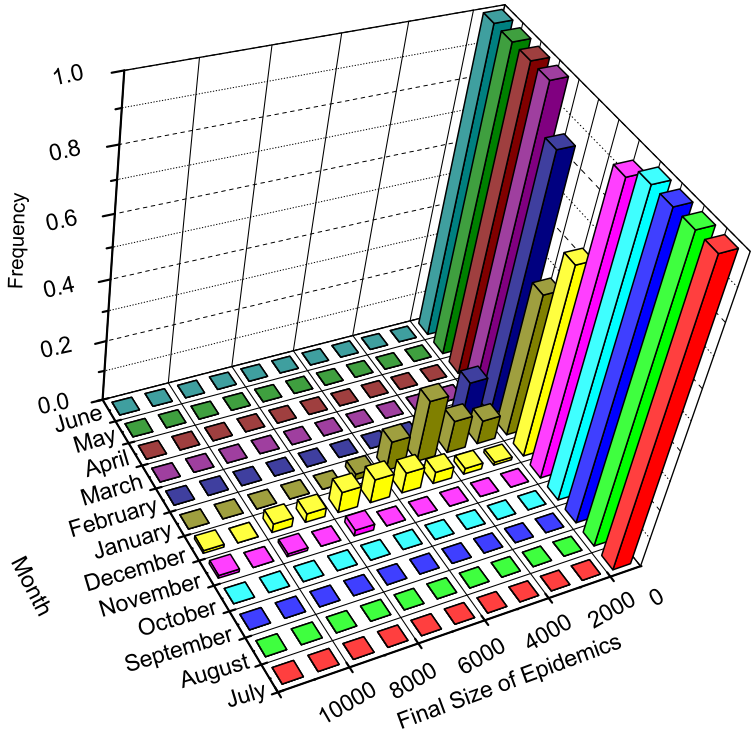

Fig. 3. Histograms of final size of epidemics vs. date of arrival of one exposed human in the susceptible population for simulations with 200 BS/patch and an initial population of 100 susceptible humans/patch.

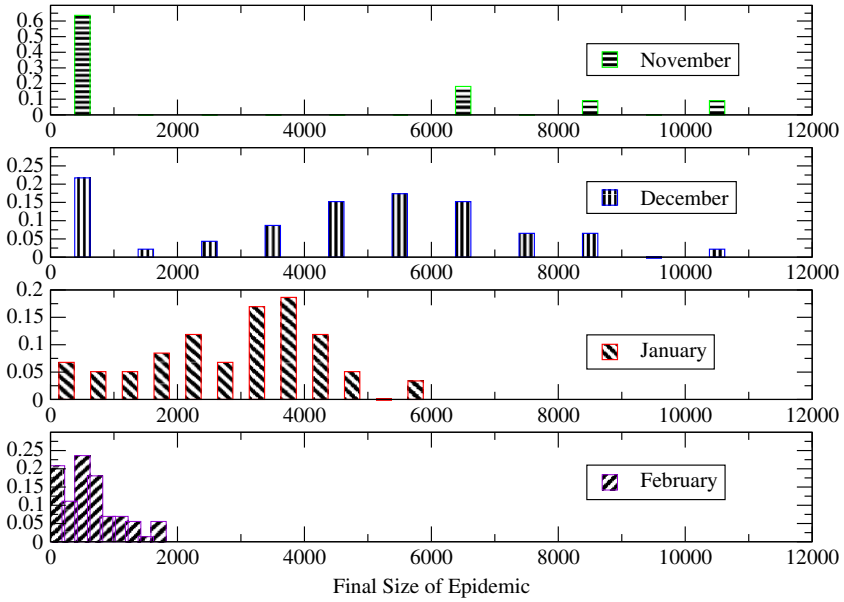

Fig. 4. Relative frequency of non-zero final size of epidemics for different dates of arrival of the exposed human in the susceptible population for simulations with 200 BS/patch, an initial population of 100 susceptible humans/patch and dates of arrival of the exposed human: November 1st, December 1st, January 1st and February 1st.

outbreak is low but in case of an outbreak the consequences are of sanitary emergency. By comparing the four histograms it can be seen that the later the date of arrival of the exposed human during the summer season, the lower the centers of the final size distribution. In order to understand the underlying processes that determine this behavior, we compared the temporal dynamics of the infectious population with the temporal dynamics of the mosquitoes (Fig. 5).

Fig. 5A shows the evolution of the infectious human population under the conditions already described, initial human population of 100 susceptible humans/patch and four different dates of arrival of the exposed human: November 1st, December 1st, January 1st and February 1st. The infectious human population profiles correspond to typical results belonging to final sizes of the center of the distributions. Fig. 5 B shows the temporal dynamics of the adult females per patch.

As it was already observed in Fig. 4, outbreaks starting with the arrival of the exposed human in late spring (November 1st) will have a lower chance to evolve, but those that eventually develop are likely to produce large epidemic outbreaks (Fig. 5A) because they have a longer time to evolve until the disappearance of the adult vector population at the beginning of the winter season (Fig. 5B). A later arrival of the exposed human (December 1st to February 1st) produces outbreaks with lower populations of infectious humans because in all the cases studied the end of the epidemics was not due to the depletion of the susceptible humans but rather to the extinction of the mosquitoes by the end of fall

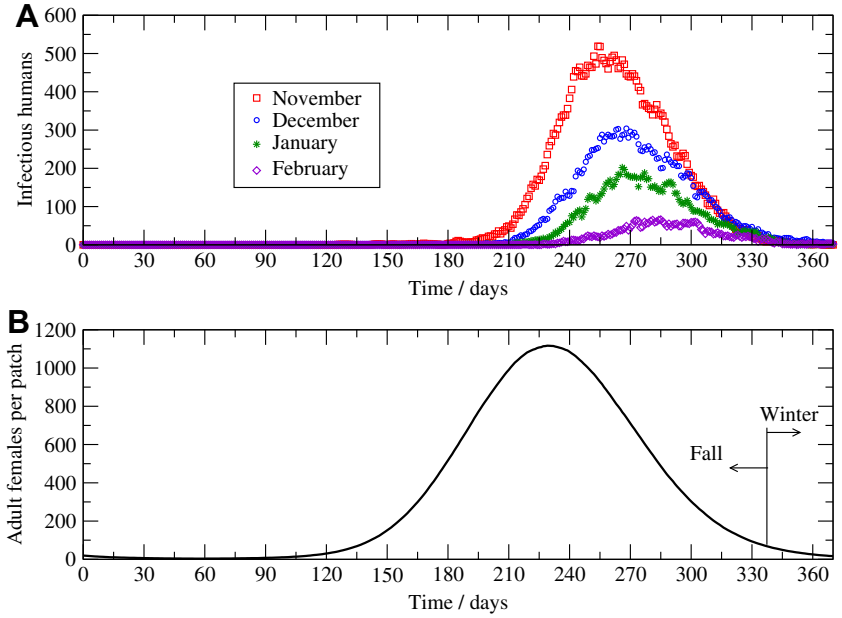

Fig. 5. Temporal evolution of the Infectious human population and the adult female vector population per patch for simulations with 200 BS/patch and for four different dates of arrival of the exposed human: November 1st, December 1st, January 1st and February 1st.

and the beginning of winter. That means that the beginning of the outbreak influences the dynamics of the disease and the final size of the epidemic, being the end of the epidemic modulated by the mosquito seasonal dynamics.

While Fig. 5A shows the temporal dynamics of the infectious populations, Fig. 6 shows the spatio-temporal evolution of the infectious human population during an outbreak for a grid of 13×13 patches, 200 BS/patch and an initial population of 100 susceptible humans per patch. The outbreak is originated by the arrival of one exposed human on January 1st at the central patch of the grid. Fig. 6 shows four pictures that represent four different moments of the outbreak (considering January 1st as $day = 0$): the early stages of the epidemic outbreak, characterized by the appearance of the first secondary infectious humans in the central and surrounding patches (day 25), the development of an epidemic focus in the center of the grid (day 60), the decrease in the infectious population in the center of the patch because of recovery and the spread of the disease in all directions resembling a cylindrical travelling wave in a reacto-diffusion model (day 100) and finally the last stages of the outbreak because of the extinction of the adult female mosquito population by the end of fall and the beginning of winter (day 125).

5.2. Effect of the density of breeding sites in the probability of no-development of an epidemic outbreak

Having studied the effect of the date of arrival of the exposed human, we studied the effect of the density of breeding sites. A higher density of breeding sites corresponds to a higher population of mosquitoes [17] and a possible higher probability of development of an epidemic outbreak because of the higher availability of vectors spreading the disease. In order to check this possibility, we ran a new set of simulations with different densities of breeding sites.

Fig. 7A shows the probability of no-development of an epidemic outbreak (started from only one exposed/infected human) $P(0)$ as a function of the date of arrival of the exposed human in the susceptible population for four different densities of breeding sites: 20, 50, 100 and 200 BS/patch, and Fig. 7 B shows the pupae per person ratio for 20, 50, 100 and 200 BS/patch. The probability of no-development of an epidemic outbreak $(P(0))$ was estimated by the frequency of runs with zero final size of epidemic and the pupae per person ratio (r) was estimated as the total pupal population normalized by the total human population.

In Fig. 7 we related the probability of no-development of epidemic outbreaks to the pupae per person ratio because this ratio has been used as an index of infestation and as an epidemiological indicator of dengue transmission in tropical locations [30]. This index involves the pupal population because pupae are easy to be counted and identified from other genera, pupal mortality is slight and well-characterized and finally because the density of pupae is highly correlated with the density of adults.

Fig. 7 shows that the pupae per person ratio grows with the density of breeding sites but the probability of no-development of an epidemic outbreak $(P(0))$ decreases with the density of breeding sites, being almost in phase with the pupae per person ratio. For each density of breeding sites the maximum pupae per person ratio and the minimum $P(0)$ are reached between January and March (summer and the beginning of fall).

5.3. Caution regarding the notion of epidemic thresholds

The notion of epidemic threshold has been discussed repeatedly in the literature. Its meaning is clear in terms of deterministic equations, where the loss of stability of the equilibrium representing no infected people gives rise, by standard mechanisms of bifurcation theory, to a stable (endemic) equilibrium. The threshold notion has been extended to stochastic processes using the limit of large populations where the rates associated with the stochastic process can be linearized [31,26], and the stochastic process can be approximated by a branching process. While such method gives rise to a clear operational procedure in terms of equations, it does not provide a natural criterion. The notion of threshold is usually presented as: when the introduction of one exposed/infected

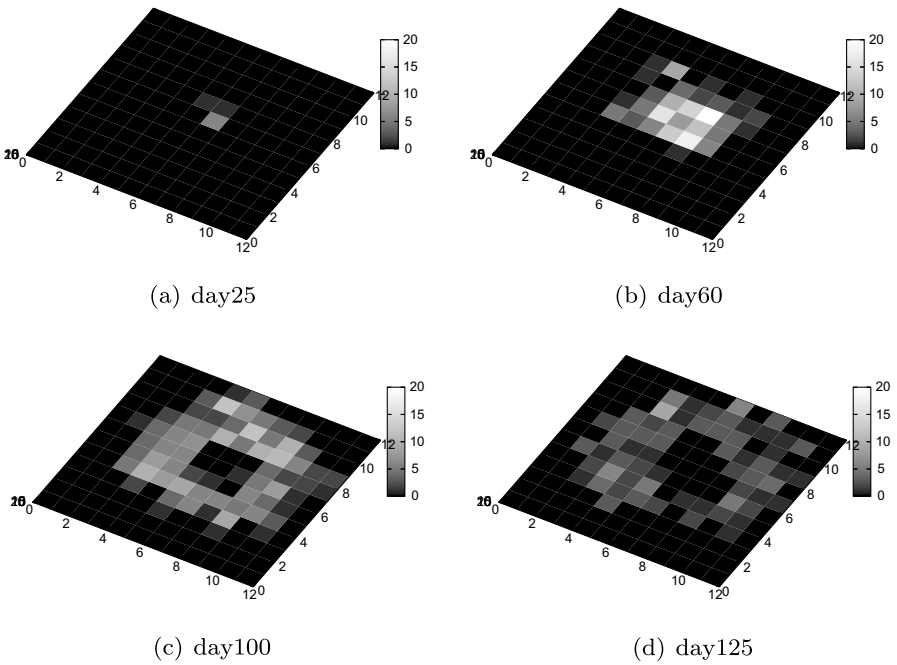

Fig. 6. Spatio-temporal evolution of the infectious human population during an outbreak for a grid of 13×13 patches, 200 BS/patch, an initial population of 100 susceptible humans per patch and the arrival of one exposed January 1st in the central patch of the grid. Four moments of the outbreak are shown: days 25, 60, 100 and 125 considering January 1st as day $= 0$.

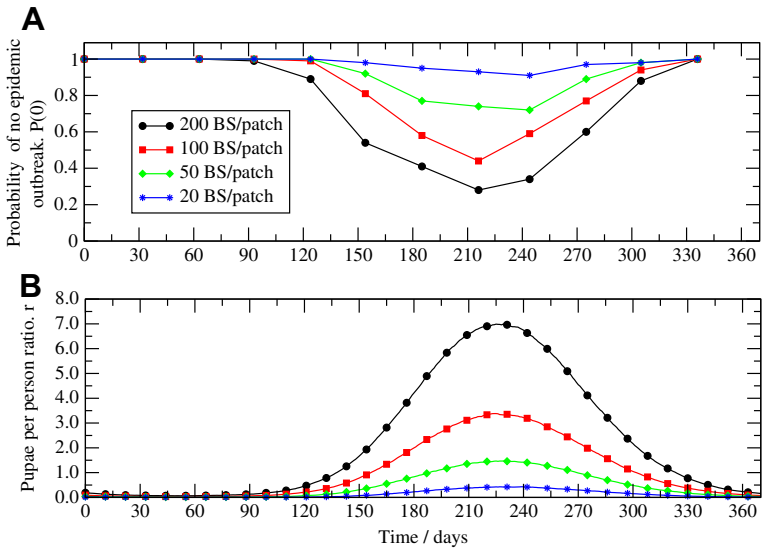

Fig. 7. Probability of no-development of an epidemic outbreak ($P(0)$) and pupae per person ratio (r) vs. the date of arrival of the exposed human in the susceptible population for different densities of breeding sites, 20, 50, 100 and 200 BS/patch.

individual into a community of susceptible individuals will not give rise to a large outbreak with probability one, the system is below threshold. The criterion is associated with the necessary use of the word "large". In natural sciences there is no "large" or "small" but rather "larger than" and "smaller than".

Nevertheless, not always the introduction of an infective human results in a major epidemic. Two epidemiological scenarios are possible, as it has been already shown in Fig. 3. Either no infection or only a few individuals will become infected or else a large proportion of the population of susceptible humans will have been infected by the end of the epidemic [26], but no clear non-arbitrary threshold can be computed from observations or simulations.

Several works have been carried out [7,8,10,13,12] in order to find a suitable expression for the basic reproductive number R_0 for dengue transmission. By R_0 we understand the average number of secondary cases arising from a single primary case in a large population of susceptible humans, and it is used as an ordinary threshold condition for the existence of an endemic state.

In 2000, Focks et al. attempted to develop dengue transmission thresholds for several dengue-endemic or dengue-receptive tropical locations in terms of the pupae per person ratio [30], and estimated this ratio in several conditions of constant temperatures and initial seroprevalences of antibodies in the population. In particular the ratio is approximately between 1 and 3 for constant temperatures between 24 and 26 degrees (according to daily mean temperatures of the city of Buenos Aires in summer) and with an initial seroprevalence of antibody of 0%.

Considering Figs. 4 and 7 jointly, we see that the epidemic outbreaks for 200 BS that start on November 1st (day 123 in Fig. 7) present about 1 pupa per human and a probability of not developing an epidemic of 0.8, but a possibility of having large epidemic outbreaks. This is not precisely a disagreement between our work and that by Focks et al., but rather a necessary consequence of seasonal effects not included in the models by Focks. Such effects not always take the form of summer-winter temperature differences, but even in tropical regions they are present as humid (rainy)-dry seasons.

According to our model, pupae per person ratios between 1 and 3 would correspond to densities between 50 and 100 BS/patch and probabilities of no-development of an epidemic outbreak $P(0)$ between 0.75 and 0.45, respectively. Differences between both models were not unexpected because even though the pupae per person ratio might be a good estimate of *A. aegypti* infestation, its use as a dengue risk index is doubtful in temperate climates where the mosquito spatio-temporal dynamics modulates the epidemic outbreaks. We have already shown that very unlikely epidemic outbreaks beginning at the end of spring could lead to large final sizes of epidemics.

In 1964, M. S. Bartlett proposed a simple analytical expression for the probability of no major epidemics started from only one infected human [31]. This probability Q^* is given by Eqs. (11) and (12). We must keep in mind that in Bartlett's model, vector populations and infection rates were considered constant (no seasonal effects) although he was inspired in malaria (a comprehensive retelling of Bartlett results can be found in [32]).

$$Q^* = \frac{\mu_1 * (\mu_2 + \lambda_1 * Sh)}{\lambda_1 * Sh(\mu_1 + \lambda_2 * Sv)} \tag{11}$$

or

$$Q^* = 1 \tag{12}$$

whichever is the smaller and where Sh is the initial population of susceptible humans, Sv is the initial population of susceptible vectors, λ_1 is the rate of infection for humans per susceptible human per infected vector, λ_2 is the rate of infection for vectors per susceptible vector and infected human and μ_1 and μ_2 are the removal rates for infected humans and vectors, respectively.

According to our model, the parameters of Bartlett's model can be expressed as: $\lambda_1 = cycle2 * avh$, $\lambda_2 = cycle1 * ahv$, $\mu_1 = (1/VP)$, $\mu_2 = ma$, $Sh = Nh_{(i,j)}$ and $Sv = Av_{(i,j)}$ which is the total adult female vector population whose dynamics are seasonal. Then a Bartlett-like estimate of $P(0)$ is given by Eqs. (13) and (14).

$$Q^* = \frac{(1/VP) * (ma + cycle2 * avh * Nh_{(i,j)})}{cycle2 * avh * Nh_{(i,j)}((1/VP) + cycle1 * ahv * Av_{(i,j)})} \tag{13}$$

or

$$Q^* = 1 \tag{14}$$

whichever is the smaller and where $cycle1$ and $cycle2$ are the gonotrophic cycle rate coefficients (see Appendix B), ahv is the transmission probability from host to vector, avh is the transmission probability from vector to host, $(ahv = avh = 0.75)$, VP is the viremic period $(VP = 3$ days$)$, ma is the mortality coefficient of

adult vectors $ma = 0.091$ days^{-1} and $Nh_{(i,j)}$ and $Av_{(i,j)}$ are the human and adult female vector populations per patch respectively.

Fig. 8 shows the $P(0)$ values obtained with our model (with 0.90 confidence intervals) vs the date of arrival of the exposed human in the susceptible population for different densities of breeding sites (20, 50, 100 and 200 BS/patch) and, for comparison, results derived from a Bartlett-like Model, Eq. (13). First, notice that the Bartlett model assumes a constant vector population, which we took as the population of the day the first infectious individual is placed. Second, Bartlett's model produces the probability of not having a major outbreak (P^*) where as already explained, major has no precise meaning, but we know that $P^* \geqslant P(0)$. Finally, Q^* is an approximation to P^* that not only simplifies the biological problem but also introduces linear rates instead of the non-linear rates of the problem. The way in which the linearization is performed disregards the slowing down (and eventually ceasing) of the epidemic outbreak by the exhaustion of susceptible individuals and saturation of exposed vectors. Since $P^* \geqslant Q^*$ and $P^* \geqslant P(0)$ the relation between Q^* and $P(0)$ is not fixed a priori.

Fig. 8 shows that for low vector densities (20 and 50 BS/patch) $Q^* > P(0)$. We see that Q^* would suggest zero probability of large epidemic outbreaks starting on November 1st or May 1st even for 200 BS/patch, although both situations are quite different. Epidemics starting on May 1st have no chance to develop into large epidemic outbreaks but those starting on November 1st can produce major outbreaks although with small frequency. When the epidemic outbreaks start near the maximum of the mosquito population (February 1st) the estimation by Eq. (13) goes from excess at 20 BS/patch to defect at 200 BS/patch corresponding to the increase in the abundance of vectors and the corresponding improved performance of the linearization. For 20 BS/patch, the predicted epidemic outbreaks starting on January 1st involve 14 cases. However, whether 14 cases represent a not-large epidemic outbreak in a region with no precedents of dengue is a matter of public policy and cannot be settled by mathematical criteria completely unrelated to public health criteria.

6. Miscellaneous discussion

6.1. Dengue and yellow fever

Dengue and yellow fever are two kinds of encephalitis that produce hemorrhagic fever. At the level of description explored in the present work they are not distinguishable, except perhaps for different characteristic times of the clinical phase and the extrinsic cycle of the virus.

From a **clinical point of view**, the main difference between dengue and yellow fever is the mortality of the toxic period. In both diseases, fever takes a saddle back pattern, with fever dropping or disappearing during some hours (up to 48 h) followed by a re-emergence [34,37]. In yellow fever, this second febrile period is called the "toxic period" and occurs in about 15–25% of the cases [33], leading to death in about half of them. The toxic period in yellow fever is not contagious and as such does not change the dynamics of the epidemic.

From a **virological point of view**, dengue and yellow fever are produced by two flaviviruses of the *Flaviviridae* family [35].

The **involved vector** in the Americas for urban yellow fever and dengue is the same mosquito: *A. aegypti* [20,36,35].

The **immunological response** to these viruses is so similar that the IgG-ELISA and hemagglutination-inhibition tests cannot distinguish between flaviviruses [37]. It has been argued that dengue could provide immunity for yellow fever, an argument that has been later proven wrong by experiments in mice [38]. Yet, chimeric dengue vaccines are being sought as modified yellow fever vaccines [39], a project that exploits similarities at the molecular level of both viruses.

All the similarities described indicate that our dengue model can be used, with a proper choice of parameters, to simulate urban yellow fever outbreaks, as discussed in [35] for simpler models.

6.2. Choice of parameters for dengue

The quantitative details of dengue transmission are not completely known, in part because clinical manifestations of dengue

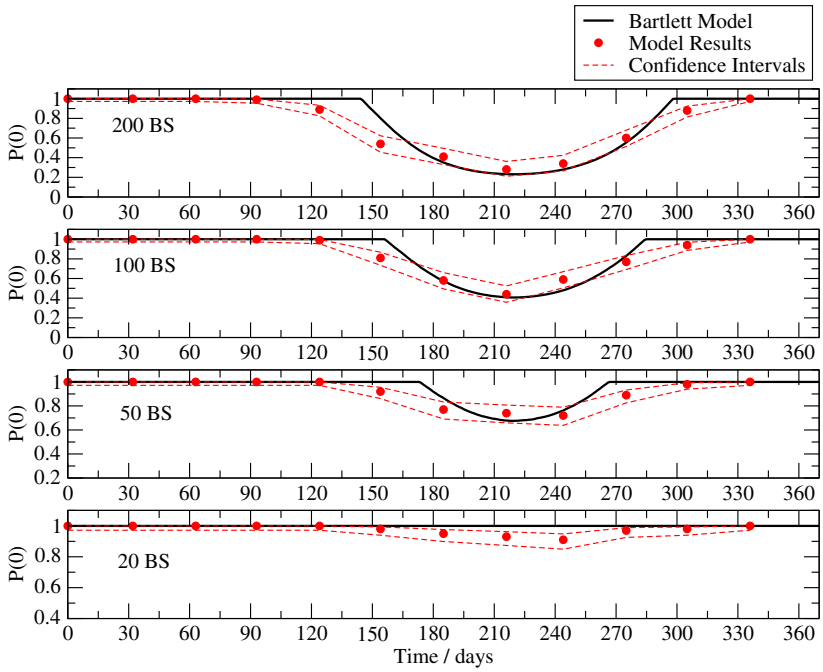

Fig. 8. Probability of no-development of an epidemic outbreak (with 0.90 confidence intervals) vs the date of arrival of the exposed human in the susceptible population for different densities of breeding sites, 20, 50, 100 and 200 BS/patch and comparison with results predicted by Bartlett Model.

do not follow immediately the inoculation of the virus by the mosquito. The acute febrile period begins after 3–14 days of inoculation [2] (Gubler reports that averages are in the range of 4–7 days [37]). During the febrile period, which lasts between 2 and 19 days, dengue viruses can circulate in the peripheral blood [[37]p484]. Since these numbers are conditioned to those people reporting dengue symptoms, thus asymptomatic and subclinical cases are not part of the sample adding more uncertainties to the description. In addition, "viremia usually peaks at the time or shortly after the onset of illness and may remain detectable for various periods ranging from 2 to 12 days" [[37], p. 487].

More uncertainties are added by the various kinds of models used for dengue. In a first group we have the stochastic models with exponentially distributed times and their deterministic limits such as in [7,9,10] and this work. These works follow Newton and Reiter [7] in their choice of parameters, with an average intrinsic incubation period of 5 days and average viremic period of 3 days.

A second set of parameters is used by Focks et al. [15]. The default value for the duration of the incubation period is of 4 days and for the duration of viremic period is of 5 days. The precise way in which this parameter is used is not clear, presumably in an accounting program (also called dynamics time table). After being infected, people enter the incubation stage and after 4 days move into the viremic phase, which lasts 5 days. To add further complexity, the transmission of virus to the biting mosquito responds to the level of viremic titer, whose form changes along the viremic period.

A third and last set of parameters is used in a deterministic model implementing the so-called linear-chain-trick [40]. In this case the mean intrinsic incubation period is of 5.5 days and the viremic period has a mean of 5 days (These averages correspond to incomplete gamma distributions associated with 54 and 25 exponentially distributed steps).

It is clear that the three families of models rely heavily on what is possible to simulate. Existing data are scarce. Experiments performed with human beings before World War II are perhaps the best source of data. Recently two of these experiments have been revisited [41].

The incubation period is defined in [41] as the time from the mosquito bite until the day of the onset of the illness (i.e., fever), and averages 6 days (DEN4) and 5.7 days (DEN1) with cases as early as 3 days and as late as 10 days. The viremic period is counted from the onset of classical dengue symptoms (day zero) and extends from −2 to 3 days (i.e., the possibility of infecting a mosquito can precede 2 days the appearance of clinical symptoms). In order to compute Virus Transmission Rates ($VTR(t)$), counting by days from the inoculation, we need to perform the convolution

$$\int_0^t \phi_{Inc}(t-s)g(s)ds \tag{15}$$

where $\phi_{Inc}(s)$ is the probability density distribution for the incubation time and $g(s)$ the probability of infecting a mosquito at the time s after the onset of the contagious period (i.e., $g(t)$ is zero for $t \notin [0, WV]$ where WV is the limit of the window for viremia). The experimental function reported in [41] has $WV = 5$ days, the accumulated weight factor of virus transmission is $W = \int_0^{WV} g(s)ds = 3.5$, the average time of incubation (i.e., before viremia) is 4 days (DEN4) and 3.7 days (DEN1) and the average transmission time is $ATT = \int_0^{WV} sg(s)ds/W$, which takes the value $ATT = 2.38$ days counting from the start of the viremic period.

The interpretation of the identified characteristics is as follows: assume that susceptible mosquitoes bite at a constant rate b and that the time is counted from the beginning of the viremic period. When $t > WV$ there are no viruses transmitted to the mosquitoes. The average number of infected mosquitoes per viremic person is then $W\,b$, while the average time when a mosquito loaded the virus is ATT. When the viremic period is exponentially distributed with parameter VP and the transmission probability from host to vector is ahv, we have $W = VP\,ah\nu$ and $ATT = VP$.

It is extremely important to notice that the incubation period as defined by Gubler [37] and by Nishiura and Halstead [41] differs in meaning with the incubation period given in modelling works including those by Focks et al. [15], Chowell et al. [40] and this work. Incubation period refers to the time from virus inoculation to fever in [37,41] and from virus inoculation to the beginning of the infective period here and in [15,40].

We summarize the results corresponding to the data and models in Table 8. Notice that the value of W will only be relevant when not only the evolution of the epidemic but also the adult mosquito population is measured, since the mosquito population (or the number of breeding sites in this work) is roughly a multiplicative factor in front of $g(s)$.

When the human viremic period is changed in the model, both ATT and W change according to the assumed exponential distribution of the viremic time. As W increases, we expect a larger proportion of mosquitoes infected and thus more circulation of the virus and larger final size of the epidemic. However, the opposite effect may occur to a lesser degree since it takes a longer average time for a mosquito to load the virus, reducing the number of contagious cycles prior to winter, and resulting in smaller outbreaks. We illustrate these effects in Fig. 9. All the plots correspond to the final size of an epidemic started with the arrival of one infected person on January 1st and correspond to an environment with *A. aegypti* sustained in the equivalent to 200 breeding sites. The plot in the center is the same plot shown in Fig. 4 for January, repeated to facilitate the comparison. On top, only the viremic period has been changed from 3 to 5 days, resulting in larger epidemics as expected. The bottom plot presents the same change in viremic period with the additional change of ahv (7) from 0.75 to 0.45 to compensate the change of W. We can see then how the effect of a longer period produces smaller epidemics when the infected mosquitoes are compensated by other parameters.

6.3. A first encounter with (real) dengue

The history of dengue in Argentina has been resumed in Appendix A, but the account in the appendix was up to the date of submission of the initial version of this work.

Between the date of the first version and that of the revised version, the largest ever epidemic of dengue in Argentina developed. With several simultaneously active focus disseminated through the country, such as in Charata, Catarmarca, Tartagal, Oran, Tucumán and other cities, dengue virus began to circulate through the country. In retrospect, the initial cases emerged at the beginning of January while the peak of the epidemic was around mid-April [42].

Table 8
Comparison of dengue transmission parameters in different works. The present work follows [7]. The values extracted from [41] are direct elaboration of experimental data. IIP = intrinsic incubation period; ATT = average time virus transmission (human to mosquito); IIP + ATT = characteristic time from onset of dengue and mosquito infection; W = accumulated weight factor of virus transmission and WV = window of viremia.

Work	IIP/days	ATT/days	I + ATT/days	W	WV/days
Newton [7]	5	3	8	2.25	—
Focks [15]	4	0–5	4–9	1.5–2.75	5
Chowell [40]	5.5	∼2.5	∼8	∼0.98	—
Nishiura [41]	4 (DEN1)	2.38	6.38	3.5	5

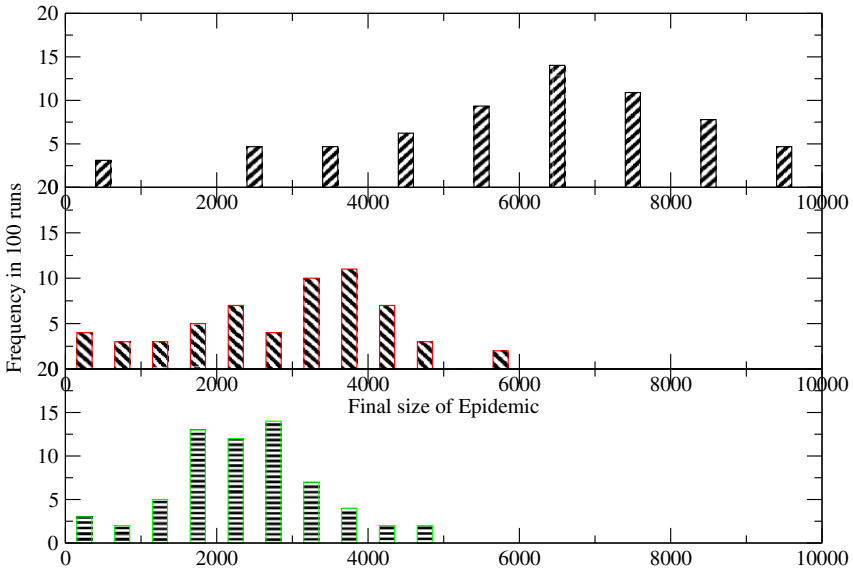

Fig. 9. Frequency of the total number of infected people in 100 simulations of epidemic outbreaks starting on January 1st for 200 breeding sites per block. Top, viremic period of 5 days (ATT = 5 days, $W = 3.75$). Middle, viremic period of 3 days (ATT = 3 days, $W = 2.25$) and bottom, viremic period of 5 days (ATT = 5 days, $W = 2.25$).

During the year, a total of 106 imported cases were confirmed in the city of Buenos Aires. However, potential local cases were routinely dismissed until the end of March enforcing the belief that dengue transmission was not possible in the region. The total of local cases confirmed so far is of 20. During the same period of time only 72 imported cases were confirmed (the geographical distribution of cases presents higher density in the quarter of Mataderos than in other regions of the city). Assuming an equal handling of local and imported cases, the ratio between local cases and total cases (R) is $R \approx \frac{20}{92} \approx 0.22$, while our computations for Mataderos (a district which has the largest recorded infestation of *A. aegypti*) are in the range: $0.05 \leqslant R \leqslant 0.76$ for infected people arriving on April 1st (see Fig. 10). The range computed corresponds to the intrinsic difficulties of estimating the number of breeding sites in the area.

While a detailed calculation is for the time being not possible since details of the information are not available, we notice that the model scales in the limit of large numbers with the number of breeding sites, provided the ratio BS/human is kept constant. In this extreme simplification, the data of the city of Buenos Aires correspond to 0.5 BS/human according to our calculations. However, data available for the great Buenos Aires area (which includes several satellite cities making a continuous urbanization) produce an estimate of $R = 0.58$ which roughly corresponds to small epidemic scenarios computed for ratios of about 1.5 BS/human. These data must be considered with extreme caution because reports of confirmed cases are still changing.

The model has then survived its first encounter with dengue transmission, being able to predict without any tuning, that the ecological conditions in the city of Buenos Aires (and its extended area) made it possible the circulation of the dengue to a limited extend, for infected people arriving by late March and early April. According to the model, the date of arrival has been crucial for this outcome and more dangerous epidemic situations would develop in case of arrivals earlier in the year.

The data made so far available by the Health authority do not make it possible a deeper analysis. We can only hope that the information will be made available in the future so that more detailed checks can be performed on the model.

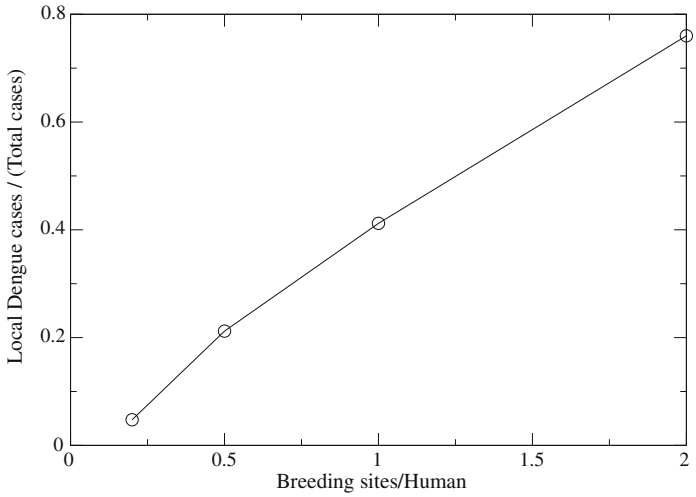

Fig. 10. Ratio between local cases and total cases in 100 runs (R) computed for different ratios of breeding sites to human beings in Mataderos.

7. Summary and conclusions

We have developed a stochastic dynamical model for the transmission of dengue that takes into account the seasonal and spatial dynamics of the vectors and describes the disease dynamics triggered by the arrival of infected people in the city and modulated by the seasonal and the spatial vector dynamics.

The model takes into account the populations of both hosts (Humans) and vectors (*A. aegypti*), which are divided into subpopulations representing the disease status: susceptible (S), exposed (E) and infectious (I) for adult female vectors and susceptible (S), exposed (E), infectious (I) and removed (R) for humans. The transmission of only one serotype of virus is considered and mechanical transmission (i.e., without amplification of the virus in the vector) is not taken into account. The evolution of the populations is considered in terms of random events with transition probabilities prescribed in terms of the mosquito biology, the disease evolution and the local environment. The model can be easily extended to other diseases propagated by *Aedes aegypti* such as yellow fever.

While any model is reductionist, we have tried to build our model avoiding as much as possible simplifying hypotheses (i.e., hypotheses with dubious biological support introduced only to render the calculations simpler). We actually intended to produce a simple but realistic model, where the different biological processes are reflected and acknowledged. Our expectation is that in case the model is shown not to agree with field research, the falsation will move up to the hypotheses and a piece of ignored or misunderstood biology will be unearthed. Despite the very large number of parameters required by the model, there are no free parameters to fit the model to the observations, not even the number of active breeding sites (BS) which are hard to evaluate but not hard to estimate.

We showed that the date of arrival of an exposed/infected human in a susceptible human population dramatically affects the distribution of the final size of the epidemics. Outbreaks starting with the arrival of the exposed in the late spring, have a lesser probability to evolve, but those that eventually develop are likely to produce large epidemic outbreaks because they have a longer time to evolve until the extinction of the adult female vector population at the beginning of winter. In the contrary, a later arrival of the exposed in summer (even if the probability of an epidemic outbreak is higher) produces outbreaks with lower populations of infectious humans because the end of the epidemics is modulated by the progressive extinction of the adult female mosquitoes by the end of the autumn season.

Furthermore, when conditions are favorable for the spreading of dengue in summer, the epidemic outbreak is quenched by the extinction of the adult female population in winter. When the location presents a seasonal dependence of climatic conditions, and one season is sufficiently adverse to the mosquito to prevent the spread of dengue, the probability of secondary cases will strongly depend on the basic reproductive number and on the time of arrival of the exposed person. Yet, even in situations below the epidemic threshold [31] not significantly large epidemics can sustain the circulation of the virus until favorable conditions for a large epidemic are reached. Seasonal climatic variations not only include temperature as considered here, but also humid-dry periods as in the cases studied in [16].

We believe that the results presented make a strong case for the necessity of predictive models as opposed to "criteria". If preventive measures are to be taken in time to be useful, and not late as quite often happens, it is necessary to predict the evolution of mosquito populations and the viral disease according to the real situation. Actually, mathematical models have the advantage of making explicit the predictive mechanism while criteria, once separated from the originating work, appear as universal conclusions, as they leave for the user the verification of hidden hypotheses.

Our model could be used as a mathematical tool to study different epidemic scenarios in urban environments and to estimate the risk and final size of epidemic outbreaks in temperate cities where seasonal temperature changes cannot be ruled out. For general use, the model needs to incorporate the dry-humid cycle. Work is in progress in this direction as well, but we anticipate that current biological knowledge on this matter is not as accurate as the knowledge of the temperature influence, and the development of an improved model runs in parallel with the development of biological understanding.

Having formulated a model that intends to be almost as realistic as possible under present knowledge of the problem, we intend to "validate" it by contrasting its results with real epidemic observations. The recent circulation of the virus in the target region will offer a good opportunity for validation. The model can be easily adapted to other regions using the appropriated climatic data, and further validation and/or tuning can be achieved in this form. Furthermore, since the model can also be easily adapted to yellow fever outbreaks (as discussed in Section 6.1), the eco-epidemiological approach supported in the description of the mosquito *A. aegypti* can be tested with the historical records of urban yellow fever epidemics. The reconstruction of the historic epidemic of 1871, with its more than 13,000 death cases will be the subject of a separate study.

The discussion regarding the choice of parameters in Section 6 indicates that compensatory effects may occur. Epidemic data may not be enough to determine, indirectly, parameter choices unless the details of the epidemic outbreak are considered and the mosquito abundance is sampled. The data recently made available by Nishiura and Halstead [41] suggest that all the existing dengue models will fail at one point or another, and that new forms of modelling are needed to achieve further realism.

Acknowledgements

The authors acknowledge CONICET and the support given by the University of Buenos Aires under Grant X308 (2004–2007), X210 (2008–2010) and by the Agencia Nacional de Promoción Científica y Tecnológica (Argentina) under Grants PICTR 87/2002 and PICT 00932/2006.

Appendix A. A brief history of dengue fever in Argentina

In 1916 an epidemic of dengue in Argentina, introduced from Paraguay, affected the cities of Concordia (Corrientes) and Paraná (Entre Rios). In 1947 the Pan-american Health organization (PHO) led a continental mosquito eradication program which consisted of the use of insecticides and the systematic destruction of water containers [43]. By 1967 the mosquito was considered to be eradicated in 18 countries including Argentina. In 1986 the mosquito was detected in Posadas, Puerto Iguazú and other cities in northern Argentina, and finally in the city of Buenos Aires by 1995. In 1997 *DEN*2 cases were detected in cities of Salta such as Orán, Salvador Mazza, Güemes and Tartagal and in 1998 an epidemic outbreak of *DEN*2 in the region of the Chaco Salteño with epicenter in the city of Tartagal caused 359 confirmed cases [44]. From December 1999 to May 2000 the Muñiz Infectology Hospital of Buenos Aires received 50 patients infected with dengue (*DEN*1) imported mainly from an extended epidemic in Paraguay [6]. In 2000 two *DEN*1 epidemic outbreaks were reported in Misiones and Formosa, both outbreaks probably originated from imported cases from neighboring endemic countries. In 2002 *DEN*3 appeared in Misiones and 214 *DEN*1 cases were detected in Salta. A total of

98 confirmed cases were reported in the country in 2003 [44], and in 2004 an extended outbreak of *DEN*3 took place in the cities of Salvador Mazza, Orán, Tartagal, Embarcación, Aguaray and Pichanal [6]. The situation in the northwestern region became worse in 2006 because of floodings mainly in the city of Tartagal. Small outbreaks took place not only in the northwestern region (Chaco Salteño) but also in the northeastern region (Iguazú), with 55 and 90 reported cases respectively.

Appendix B. Temperature model and parameter values

B.1. Temperature model

A very simple model for the mean daily temperature variation, which contains only the deterministic component of the temperatures, was used in this work. The model was chosen from [45] and takes the form:

$$T = a + b\cos\left(\frac{2\pi t}{365.25\text{days}} + c\right) \tag{16}$$

with time measured in days beginning on the first of July. The parameters *a, b* and *c* were fitted from temperature records along a period of time of 10 years and are: $a = 18.0\,^{\circ}\text{C}; b = 6.7\,^{\circ}\text{C}$ and $c = 9.2$. The use and development of this model is detailed in [17].

B.2. Developmental rate coefficients

The developmental rates that correspond to egg hatching, pupation, adult emergence and the gonotrophic cycles were evaluated using the results of the thermodynamic model developed by Sharp and DeMichele [46] and simplified by Schoofield et al. [47]. According to this model, the maturation process is controlled by only one enzyme which is active in a given temperature range and is deactivated only at high temperatures. The development is stochastic in nature and is controlled by a Poisson process with rate $R_D(T)$. In general terms $R_D(T)$ takes the form

$$R_D(T) = R_D(298\,^{\circ}\text{K}) \times \frac{(T/298\,^{\circ}\text{K}) * \exp((\Delta H_A/R)(1/298\,^{\circ}\text{K} - 1/T))}{1 + \exp(\Delta H_H/R)(1/T_{1/2} - 1/T)} \tag{17}$$

where T is the absolute temperature, ΔH_A and ΔH_H are thermodynamics enthalpies characteristic of the organism, R is the universal gas constant, and $T_{1/2}$ is the temperature when half of the enzyme is deactivated because of high temperature.

Table 9 presents the values of the different coefficients involved in the events: egg hatching, pupation, adult emergence and gonotrophic cycles. The values are taken from [48] and are discussed in [17].

Table 9
Coefficients for the enzymatic model of maturation (Eq. (17)). R_D is measured in day^{-1}, enthalpies are measured in (cal/ mol) and the temperature T is measured in absolute (Kelvin) degrees.

Develop. cycle (17)	$R_D(T)$	$R_D(298^{\circ}\text{K})$	ΔH_A	ΔH_H	$T_{1/2}$
Egg hatching	elr	0.24	10,798	100,000	14,184
Larval develop.	lpr	0.2088	26,018	55,990	304.6
Pupal develop.	par	0.384	14,931	−472,379	148
Gonotrophic c. (*A*1)	Cycle1	0.216	15,725	1,756,481	447.2
Gonotrophic c. (*A*2)	Cycle2	0.372	15,725	1,756,481	447.2

B.3. Mortality coefficients

B.3.1. Egg mortality

The mortality coefficient of eggs is **me** $= 0.011$/day, independent of temperature in the range $278\,^{\circ}\text{K} \leqslant T \leqslant 303\,^{\circ}\text{K}$ [49].

B.3.2. Larval mortality

The value of α_0 (associated with the carrying capacity of a single breeding site) is $\alpha_0 = 1.5$ and was assigned by fitting the model to observed values of immatures in the cemeteries of Buenos Aires [17]. The temperature-dependent larval death coefficient is approximated by $\mathbf{ml} = 0.01 + 0.9725\exp(-(T - 278)/2.7035)$ and is valid in the range $278\,^{\circ}\text{K} \leqslant T \leqslant 303\,^{\circ}\text{K}$ [50–52].

B.3.3. Pupal mortality

The intrinsic mortality of a pupa has been considered as $\mathbf{mp} = 0.01 + 0.9725exp(-(T - 278)/2.7035)$ [50–52]. Besides the daily mortality in the pupal stage, there is an additional mortality associated with the emergence of the adults. We consider a mortality of 17% of the pupae at this event, which is added to the mortality rate of pupae, hence the emergence factor is **ef** $= 0.83$ [19].

B.3.4. Adult mortality

Adult mortality coefficient is **ma** $= 0.091$/day and is considered independent of temperature in the range $278\,^{\circ}\text{K} \leqslant T \leqslant 303\,^{\circ}\text{K}$ [50,20,53].

B.4. Fecundity and oviposition coefficient

Females lay a number of eggs that is roughly proportional to their body weight (46.5 eggs/mg) [54,55]. Considering that the mean weight of a three-day-old female is 1.35 mg [20], we estimate the average number of eggs laid in one oviposition as **egn** $= 63$.

The oviposition coefficient $ovr_{(i,j)}$ depends on breeding site density $BS_{(i,j)}$ and is defined as:

$$ovr_{(i,j)} = \begin{cases} \theta/tdep & \text{if } BS_{(i,j)} \leqslant 150 \\ 1/tdep & \text{if } BS_{(i,j)} > 150 \end{cases} \tag{18}$$

where θ was chosen as $\theta = BS_{(i,j)}/150$, a linear function of the density of breeding sites [18].

B.5. Dispersal coefficient

We chose a diffusion-like coefficient of **diff** = 830 m2/day which corresponds to a short dispersal, approximately a mean dispersal of 30 m in one day, in agreement with short dispersal experiments and field studies analyzed in detail in our previous article [18].

References

[1] M. Hunt, Microbiology and Immunology On-line, University of South Carolina, School of Medicine, South Carolina, United States, 2007, Available from <http://www.med.sc.edu:85/mhunt/arbo.htm>.
[2] WHO, Dengue hemorrhagic fever, in: Diagnosis Treatment Prevention and Control, second ed., World Health Organization, Ginebra, Suiza, 1998.
[3] N. Schweigmann, R. Boffi, *Aedes aegypti* y aedes albopictus: Situación entomológica en la región, in: Temas de Zoonosis y Enfermedades Emergentes, Segundo Cong. Argent. de Zoonosis y Primer Cong. Argent. y Lationoamer. de Enf. Emerg. y Asociación Argentina de Zoonosis, Buenos Aires, 1998, p. 259.
[4] A.B. de Garín, R.A. Bejarán, A.E. Carbajo, S.C. de Casas, N.J. Schweigmann, Atmospheric control of *Aedes aegypti* populations in buenos aires (argentina) and its variability, International Journal of Biometerology 44 (2000) 148.
[5] A.E. Carbajo, N. Schweigmann, S.I. Curto, A. de Garín, R. Bejarán, Dengue transmission risk maps of argentina, Tropical Medicine and International Health 6 (3) (2001) 170.
[6] A. Seijo, Situación del dengue en la argentina, Boletín de la Asociación Argentina de Microbiología 175 (2007) 1.

[7] E.A.C. Newton, P. Reiter, A model of the transmission of dengue fever with an evaluation of the impact of ultra-low volume (ulv) insecticide applications on dengue epidemics, American Journal of Tropical Medicinal Hygiene 47 (1992) 709.
[8] L. Esteva, C. Vargas, Analysis of a dengue disease transmission model, Mathematical Biosciences 150 (1998) 131.
[9] L. Esteva, C. Vargas, A model for dengue disease with variable human population, Journal of Mathematical Biology 38 (1999) 220.
[10] L. Esteva, C. Vargas, Influence of vertical and mechanical transmission on the dynamics of dengue disease, Mathematical Biosciences 167 (2000) 51.
[11] L.M. Bartley, C.A. Donnelly, G.P. Garnett, The seasonal pattern of dengue in endemic areas: mathematical models of mechanisms, Transactions of the Royal Society of Tropical Medicine and Hygiene 96 (2002) 387.
[12] P. Pongsumpun, I.M. Tang, Transmission of dengue hemorrhagic fever in an age structured population, Mathematical and Computer Modelling 37 (2003) 949.
[13] M. Derouich, A. Boutayeb, E.H. Twizell, A model of dengue fever, Biomedical Engineering Online 2 (2003) 4.
[14] A. Tran, M. Raffy, On the dynamics of dengue epidemics from large-scale information, Theoretical Population Biology 69 (2006) 3.
[15] D.A. Focks, D.C. Haile, E. Daniels, D. Keesling, A simulation model of the epidemiology of urban dengue fever: literature analysis, model development, preliminary validation and samples of simulation results, American Journal of Tropical Medicinal Hygiene 53 (1995) 489.
[16] L.B.L. Santos, M.C. Costa, S.T.R. Pinho, R.F.S. Andrade, F.R. Barreto, M.G. Teixeira, M.L. Barreto, Periodic forcing in a three level cellular automata model for a vector transmitted disease, arXiv:0810.0384v1, 2008.
[17] M. Otero, H.G. Solari, N. Schweigmann, A stochastic population dynamic model for *Aedes aegypti*: formulation and application to a city with temperate climate, Bulletin of the Mathematical Biology 68 (2006) 1945.
[18] M. Otero, N. Schweigmann, H.G. Solari, A stochastic spatial dynamical model for *Aedes aegypti*, Bulletin of Mathematical Biology 70 (2008) 1297.
[19] T.R.E. Southwood, G. Murdie, M. Yasuno, R.J. Tonn, P.M. Reader, Studies on the life budget of *Aedes aegypti* in wat samphaya Bangkok Thailand, Bulletin of the World Health Organisation 46 (1972) 211.
[20] R. Christophers, *Aedes aegypti* (L.), the yellow fever mosquito, Cambridge University Press, Cambridge, 1960.
[21] A.E. Carbajo, S.I. Curto, N. Schweigmann, Spatial distribution pattern of oviposition in the mosquito *Aedes aegypti* in relation to urbanization in buenos aires: southern fringe bionomics of an introduced vector, Medical and Veterinary Entomology 20 (2006) 209.
[22] M. Wolfinsohn, R. Galun, A method for determining the flight range of *Aedes aegypti* (linn.), Bullentin of the Research Council of Israel 2 (1953) 433.
[23] P. Reiter, M.A. Amador, R.A. Anderson, G.G. Clark, Short report: dispersal of *Aedes aegypti* in an urban area after blood feeding as demonstrated by rubidium-marked eggs, American Journal of Tropical Medicinal Hygiene 52 (1995) 177.
[24] J.D. Edman, T.W. Scott, A. Costero, A.C. Morrison, L.C. Harrington, G.G. Clark, *Aedes aegypti* (diptera culicidae) movement influenced by availability of oviposition sites, Journal of Medicinal Entomology 35 (4) (1998) 578.
[25] S.N. Ethier, T.G. Kurtz, Markov Processes, John Wiley and Sons, New York, 1986.
[26] H. Andersson, T. Britton, Stochastic epidemic models and their statistical analysis, Lecture Notes in Statistics, vol. 151, Springer-Verlag, Berlin, 2000.
[27] H.G. Solari, M.A. Natiello, Stochastic population dynamics: the poisson approximation, Physical Review E 67 (2003) 031918.
[28] J.P. Aparicio, H.G. Solari, Population dynamics: a Poissonian approximation and its relation to the langevin process, Physical Review Letters 86 (2001) 4183.
[29] A.E. Carbajo, S.M. Gomez, S.I. Curto, N. Schweigmann, Variación espacio temporal del riesgo de transmisión de dengue en la ciudad de buenos aires, Medicina 64 (2004) 231.
[30] D.A. Focks, R.J. Brenner, J. Hayes, E. Daniels, Transmission thresholds for dengue in terms of *Aedes aegypti* pupae per person with discussion of their utility in source reduction efforts, American Journal of Tropical Medicinal Hygiene 62 (1) (2000) 11.
[31] M.S. Bartlett, The relevance of stochastic models for large-scale epidemiological phenomena, Applied Statistics 13 (1) (1964) 2.
[32] A.L. Lloyd, J. Zhang, A.M. Root, Stochasticity and heterogeneity in host vector models, Interface 4 (2007) 851.
[33] WHO, Yellow Fever, World Health Organization, Ginebra, Suiza, 2001, fact sheet 100.
[34] J.S. Simmons, Dengue fever, The American Journal of Tropical Medicine XI (1933) 77.
[35] E. Massad, F.A.B. Coutnho, M.N. Burattini, L.F.F. Lopez, The risk of yellow fever in a dengue-infested area, Transactions of the Royal Society of Tropical Medicine and Hygiene 95 (2001) 370.
[36] P.N. Dégallier, J.P. Hervé, A.F.A.T.D. Rosa, G.C. Sa, *Aedes aegypti* (l.): Importance de sa bioécologie dans la transmission de la dengue et des autres arbobirus, Bulletin des Societes Pathologie Exotique 81 (1988) 97.
[37] D.J. Gubler, Dengue and dengue hemorrhagic fever, Clinical Microbiology Review 11 (1998) 480.
[38] J. Vainio, F. Cutts, Yellow fever, Tech. Rep., World Health Organization, Geneva, 1998.
[39] R.G. van der Most, K. Murali-JKrishna, R. Ahmed, J.H. Strauss, Chimeric yellow fever/dengue virus as a candidate dengue vaccine: quantitation of the dengue virus-specific cd8 t-cell response, Journal of Virology 74 (2000) 8094.
[40] G. Chowella, P. Diaz-Dueñas, J. Miller, A. Alcazar-Velazco, J. Hyman, P. Fenimore, C. Castillo-Chavez, Estimation of the reproduction number of dengue fever from spatial epidemic, Mathematical Biosciences 208 (2007) 571.
[41] H. Nishiura, S.B. Halstead, Natural history of dengue virus (denv)-1 and denv-4 infections: Reanalysis pf classic studies, Journal of Infectious Diseases 195 (2007) 1007.
[42] Actualización casos de dengue en argentina, 10 de mayo de 2009, Tech. rep., Ministerio de Salud Pública de Argentina, Buenos Aires, 2009, Available from <http://www.msal.gov.ar/htm/Site/sala_situacion/index.asp>.
[43] Campaña de erradicacion del *Aedes aegypti* en la república argentina. informe final, Tech. Rep., Ministerio de Asistencia Social y Salud Publica, Argentina, Buenos Aires, 1964.
[44] C. Rotela, F. Fouque, M. Lamfri, P. Sabatier, V. Introini, M. Zaidenberg, C. Scavuzzo, Space-time analysis of the dengue spreading dynamics in the 2004 tartagal outbreak northern argentina, Acta Tropica 103 (2007) 1.
[45] A. Király, I.M. Jánosi, Stochastic modelling of daily temperature fluctuations, Physical Review E 65 (2002) 051102.
[46] P.J.H. Sharpe, D.W. DeMichele, Reaction kinetics of poikilotherm development, Journal of Theoretical Biology 64 (1977) 649.
[47] R.M. Schoofield, P.J.H. Sharpe, C.E. Magnuson, Non-linear regression of biological temperature-dependent rate models based on absolute reaction-rate theory, Journal of Theoretical Biology 88 (1981) 719.
[48] D.A. Focks, D.C. Haile, E. Daniels, G.A. Moun, Dynamics life table model for *Aedes aegypti*: analysis of the literature and model development, Journal of Medical Entomology 30 (1993) 1003.
[49] M. Trpis, Dry season survival of *Aedes aegypti* eggs in various breeding sites in the dar salaam area, tanzania, Bulletin of the World Health Organisaion 47 (1972) 433.
[50] W.R. Horsfall, Mosquitoes: Their Bionomics and Relation to Disease, Ronald, New York, USA, 1955.
[51] M. Bar-Zeev, The effect of temperature on the growth rate and survival of the immature stages of *Aedes aegypti*, Bulletin of the Entomological Research 49 (1958) 157.
[52] L.M. Rueda, K.J. Patel, R.C. Axtell, R.E. Stinner, Temperature-dependent development and survival rates of culex quinquefasciatus and *Aedes aegypti* (diptera: Culicidae), Journal of Medicinal Entomology 27 (1990) 892.
[53] R.W. Fay, The biology and bionomics of *Aedes aegypti* in the laboratory, Mosquito News 24 (1964) 300.
[54] M. Bar-Zeev, The effect of density on the larvae of a mosquito and its influence on fecundity, Bulletin of the Research Council Israel 6B (1957) 220.
[55] J.K. Nayar, D.M. Sauerman, The effects of nutrition on survival and fecundity in florida mosquitoes. part 3. utilization of blood and sugar for fecundity, Journal of Medicinal Entomology 12 (1975) 220.